FLEXIBLE AIRCRAFT FLYING AND RIDE QUALITIES

Irving L. Ashkenas, Raymond E. Magdaleno, and Duane T. McRuer
Systems Technology, Incorporated
Hawthorne, California

First Annual NASA Aircraft Controls Workshop
NASA Langley Research Center
Hampton, Virginia
October 25-27, 1983

REPORT CONTENTS

This presentation covers some of the highlights of NASA CR-172201, "Flight Control and Analysis Methods for Studying Flying and Ride Qualities of Flexible Transport Aircraft." The report itself contains the chapters listed in Fig. 1, and we'll follow this order in our discussion. Of course, we'll have to limit ourselves to the more significant aspects and forego many of the details that are in the report.

We'll start with a block diagram representative of a generalized FCS, go into a brief analytic exposition to illustrate a central principle in flexible mode control, list and discuss some of the pertinent pilot-centered requirements, expose the desired features of the control methodology, and select the methodology to be used.

Then we'll discuss the example Boeing-supplied characteristics and show how we approximated these with a reduced-order model and a simplified treatment of unsteady aerodynamics. The closed-loop flight control system design follows, along with first-level assessments of resulting handling and ride quality characteristics. Some of these do not meet the postulated requirements and remain problems to be solved possibly by further analysis or future simulation.

Figure 1

GENERALIZED FLIGHT CONTROL SYSTEM FOR TRANSPORT AIRCRAFT
INCLUDING FLEXIBLE MODES

This block diagram (Fig. 2) illustrates primarily the multiple feedback paths acting on the sensor array and the possible use of secondary control points and limited forward loop elements. The primary FCS design task, of course, is to formulate the sensor equalization complex to yield a stable, robust system which meets the direct and implied requirements.

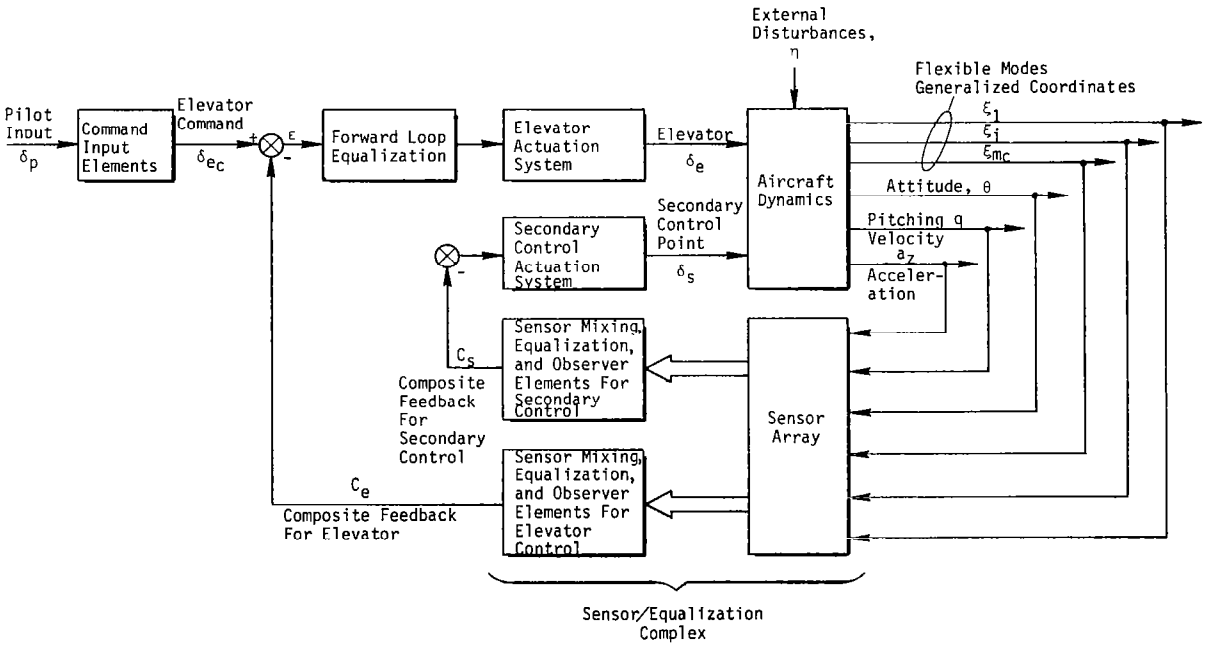

Figure 2

These equations (Fig. 3) constitute a simplified treatment of the considerations involved in synthesizing a suitable sensor-equalization response.

The first equation represents the rigid-body attitude rate response; the second is the first oscillatory flexible mode response where ϕ' is the slope of the first bending mode at the sensor station.

Adding these responses yields the third equation with the simplified numerator/denominator ratios shown. The point is that selection of the sensor location and corresponding mode slope ϕ' can be used to directly affect these ratios or the equivalent pole-zero ordering.

$$\frac{q_o}{\delta_e} \cdot \frac{\phi_o'}{s}$$

$$\frac{q_{flex}}{\delta_e} \sim \frac{\phi_1'(x)s}{s^2 + 2(\zeta_\omega)_D s + \omega_D^2}$$

$$G(s) = \frac{C_e}{E} = \frac{K[s^2 + 2\zeta_N\omega_N s + \omega_N^2]}{s[s^2 + 2\zeta_D\omega_D s + \omega_D^2]}$$

$$\omega_N = \sqrt{\frac{\phi_o'}{\phi_o' + \phi_1'}}\,\omega_D$$

$$\zeta_N = \sqrt{\frac{\phi_o'}{\phi_o' + \phi_1'}}\,\zeta_D$$

Figure 3

If the zero is greater than the pole, the root locus progresses into the right half-plane as in a); if less, it stays in the left half-plane as in b) and the proper choice of feedback gain will then provide enhanced structural mode damping.

This is a simplified explanation of a well-known general principle of flexible mode control, i.e., the desirability of synthesizing a sensor-equalization characteristic which exhibits an alternating numerator/denominator ordering of quadratic pairs (a sawtooth Bode) which creates leading phase "blips" for those modes which are to be controlled. For those modes which are to be largely ignored by the control system, appropriate notch or low-pass filtering might be considered if the modes are not so high in frequency relative to actuator and other dynamics as to make them insignificant anyway. (See Fig. 4.)

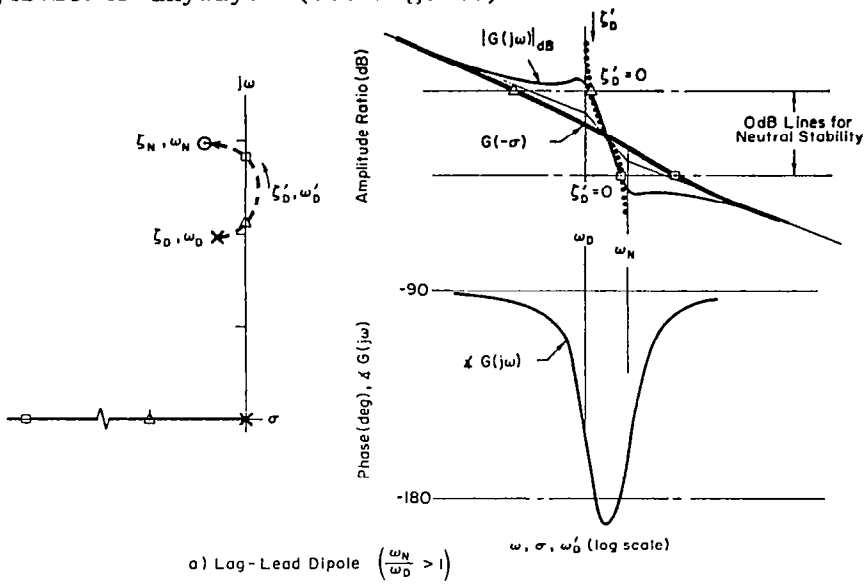

a) Lag-Lead Dipole $\left(\frac{\omega_N}{\omega_D} > 1\right)$

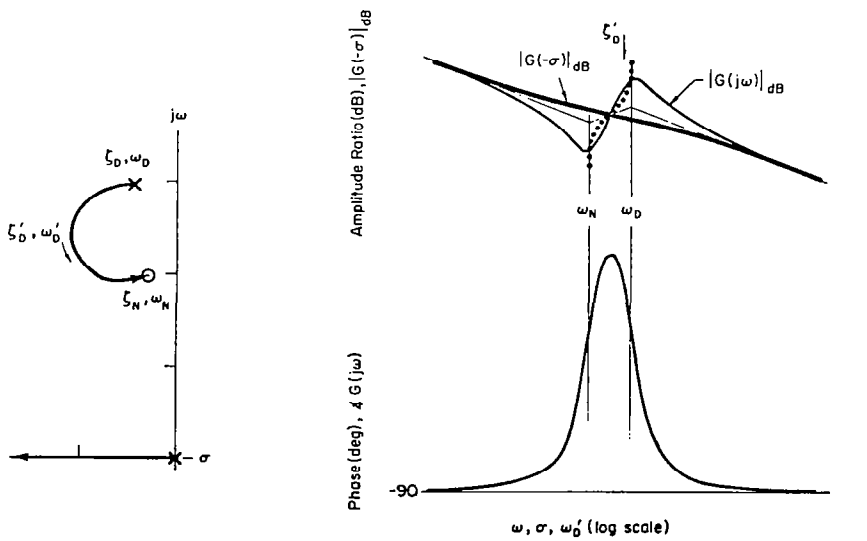

b) Lead-Lag Dipole $\left(\frac{\omega_N}{\omega_D} < 1\right)$

Figure 4

PILOT-CENTERED COMMAND REQUIREMENTS AND FLYING QUALITIES

In addition to the foregoing implied requirement, there are direct requirements for minimum satisfactory flying and ride qualities. The flying qualities list shown here pertains to pilot's attitude and acceleration response to elevator input (Fig. 5).

The first two headings refer primarily to attitude control and reflect the possible use of either frequency- or time-domain assessment criteria.

The third heading relates mostly to unwanted acceleration responses which can be excited directly by the pilot's remnant, self-excited by feedthrough to, and amplification resulting from, the pilot's body-arm-controller induced motions, or directly excited by normal closed-loop piloted operation.

The final heading generally relates to either attitude or acceleration responses, although attitude is the more common culprit. Both synchronous behavior and the PIO syndrome are assessed later for the derived system, as are pertinent aspects of the preceding items.

FREQUENCY DOMAIN

EQUIVALENT $\frac{\theta}{\delta}(s) = \frac{M_\delta(s+1/T_{\theta_2})e^{-\tau s}}{s(s^2+2\zeta\omega s+\omega^2)}$

BANDWIDTH

CLOSED LOOP

TIME DOMAIN

ENVELOPE

BOUNDED TIME PARAMETERS

TRP

FLEXIBLE MODE EFFECTS

REMNANT EXCITATION

VIBRATION FEEDTHROUGH

PILOT CLOSED-LOOP EXCITATON OF FLEX MODES

PIO CONSIDERATIONS

SYNCHRONOUS BEHAVIOR

PIO SYNDROME

Figure 5

FQ AND FLEX A/C CONTROL CONSIDERATIONS GOVERNING CONTROL DESIGN TECHNIQUE SELECTION

The summation of certain of the foregoing and of the more complete considerations in the report as they pertain to the selection of appropriate design methodology is listed here (Fig. 6).

In the first place, we have to consider uncertainties and variations in the airframe poles and zeros due to changes in flight conditions and loading.

Second, we have to utilize and consider many elements which are basically expressed in frequency-domain formulations.

Third are the direct and implied control design criteria which can be in time- or frequency-domain formulations, or simply expressed as desirable qualities.

Based on these and other considerations, the basic control methodology selected comprises conventional, classical, multivariable, frequency-domain analysis techniques.

1. KEY AIRCRAFT PARAMETERS

   POLES, ZEROS { WIDE RANGING (LO FREQ)
                { NARROW RANGES (HI FREQ)

2. FREQUENCY DOMAIN FORMULATIONS
   - PILOT I/O CONTROL ACTIVITIES, REMNANT, VIBRATION FEEDTHROUGH, PIO BEHAVIOR
   - UNSTEADY AERODYNAMICS
   - MODAL FORMULATIONS → FREQUENCY-IDENTIFIED POLES AND ZEROS
   - CONTROL ACTIVITY RANGE
   - RIDE AND HABITABILITY CONSIDERATIONS AND CRITERIA
   - RANDOM GUST INPUTS

3. CONTROL SYSTEM DESIGN CRITERIA
   - FLYING QUALITIES REQUIREMENTS
   - FLEX MODE POLE, ZERO SEQUENCING FOR CONTROLLED MODES
   - GAIN STABILIZATION FOR IGNORED MODES
   - ENHANCED DAMPING FOR MODES POSSIBLY CAUSING EXCESSIVE REMNANT PILOT FEEDTHROUGH, PILOT SYNCHRONOUS BEHAVIOR
   - PIO SUSCEPTIBILITY
   - CONTROLLER SIMPLICITY
   - CONTROLLER ROBUSTNESS

Figure 6

THREE VIEWS OF SUPERSONIC CRUISE AIRCRAFT

Before applying these techniques, it was necessary to derive a simplified representation of the Boeing-supplied data base for the delta wing supersonic cruise aircraft (SCRA), shown in Fig. 7, which included:

a. Modal equations of motion (EOM) - 25 × 25

b. Computer printouts of EOM matrix elements for 6 reduced-frequency sets of unsteady aerodynamics for each of 4 flight conditions

c. Mode shape data in a variety of formats: tabulated, interpolated displacements and slopes at selected locations on the fuselage centerline; pictorial or perspective views; and contour plots for wing relative displacements out-of-plane

d. Numerical frequency response data at 149 discrete frequencies supplied on magnetic tapes for four flight conditions. These "data" are the result of interpolation among the 6 reduced-frequency sets of unsteady aerodynamics

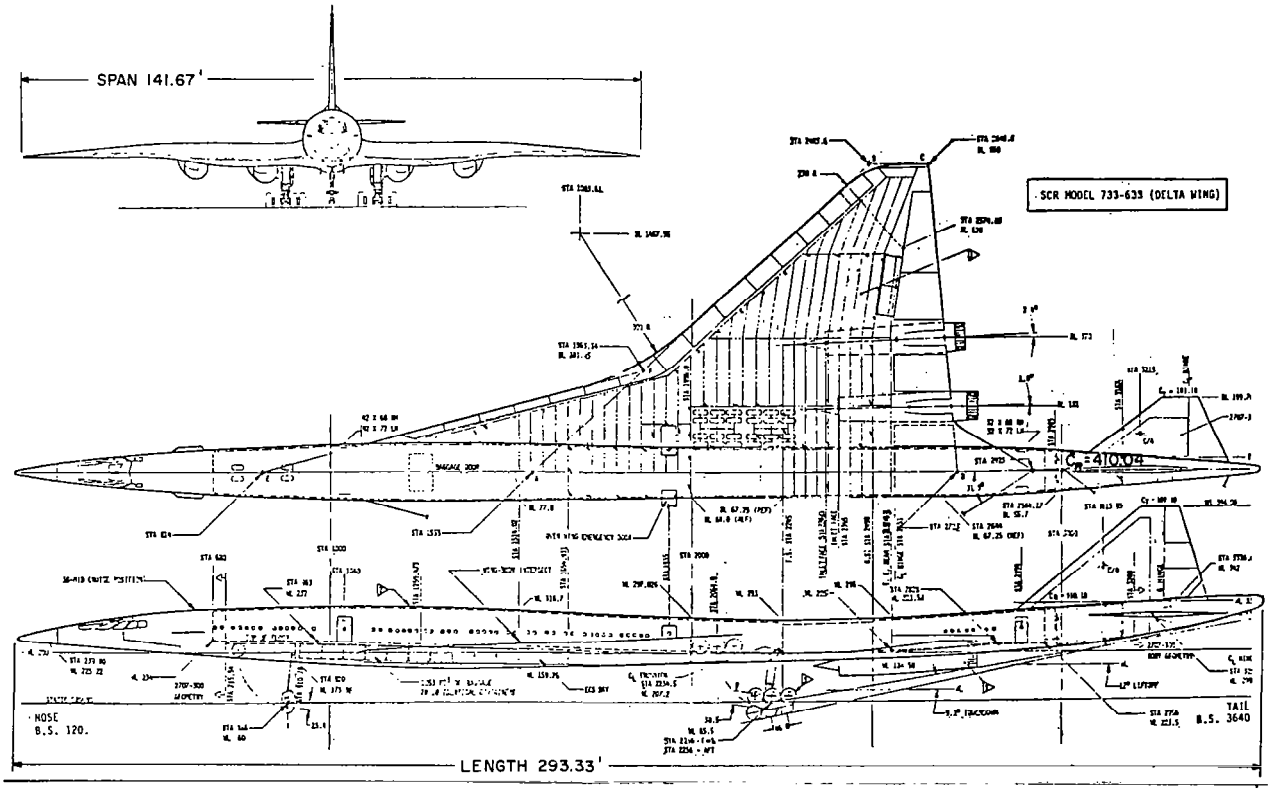

Figure 7

MODE SHAPES FOR TAKEOFF WEIGHT DISTRIBUTION

To afford an appreciation for the scope of the complete model formulation, the total set of centerline elastic mode shapes for the take-off case is shown in Fig. 8 in the form of displacement normalized to maximum deflection. In general, the modes are 3-dimensional, and Fig. 8 shows just the cut along the fuselage centerline. In many cases the maximum deflection is not along the centerline, and there is no corresponding unity value shown for those modes.

Modes one and two (Fig. 8) are rigid-body modes, respectively heave and pitching motion. Mode three is the first structural (bending) mode, and the structural modes go up in complexity and frequency as the numbers go up. The in-vacuo frequencies in Hz are as follows.

Mode	Frequency (Hz)	Mode	Frequency (Hz)	Mode	Frequency (Hz)
3	1.14	9	4.44	15	6.44
4	1.60	10	4.82	16	6.89
5	2.49	11	5.15	17	7.06
6	2.95	12	5.45	18	7.24
7	3.81	13	5.92	19	7.44
8	4.28	14	6.11	20	7.56

For a transport aircraft, this list has a remarkably large number of low-frequency closely spaced modes which can interfere, in one way or another, with piloted control.

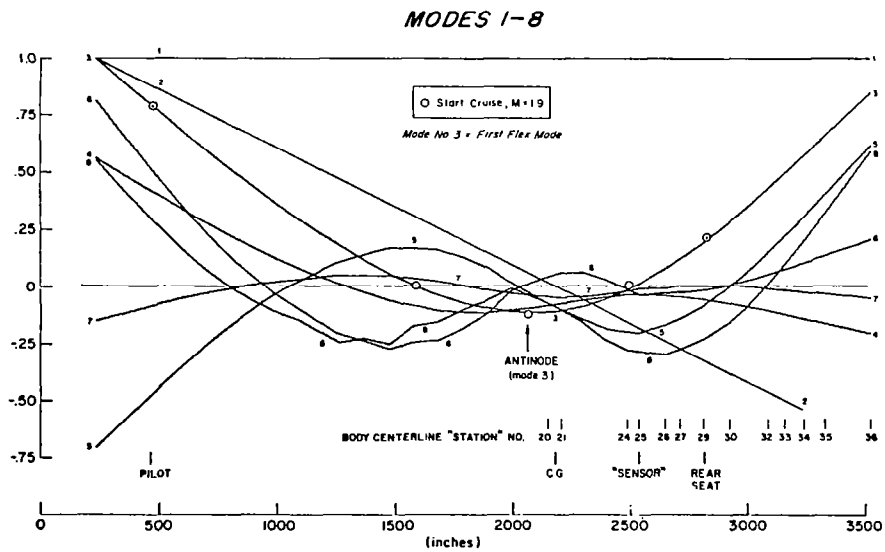

Figure 8

Various body centerline stations and physical points are identified along the bottom of each plot. The "sensor station" is one chosen by Boeing as being in a fairly stiff region as evident by the fairly flat shape of the various modes in this area. The open circle symbols in Fig. 8 show that there is little change in mode three for the start cruise condition.

Modes nine through fourteen in Fig. 9 are characterized by more lumps and bumps than the first set, and modes fifteen through twenty in Fig. 9 are even lumpier and include some very large spikes. These anomalies appear to be due to ill-conditioned lumped parameters, that is, the mass and stiffness elements chosen for the analysis are not necessarily well conditioned and apparently lead to local resonances which give rise to the discontinuities shown.

However, notice that the area in the "sensor" region, where the structure is relatively stiff, is pretty smooth for all modes.

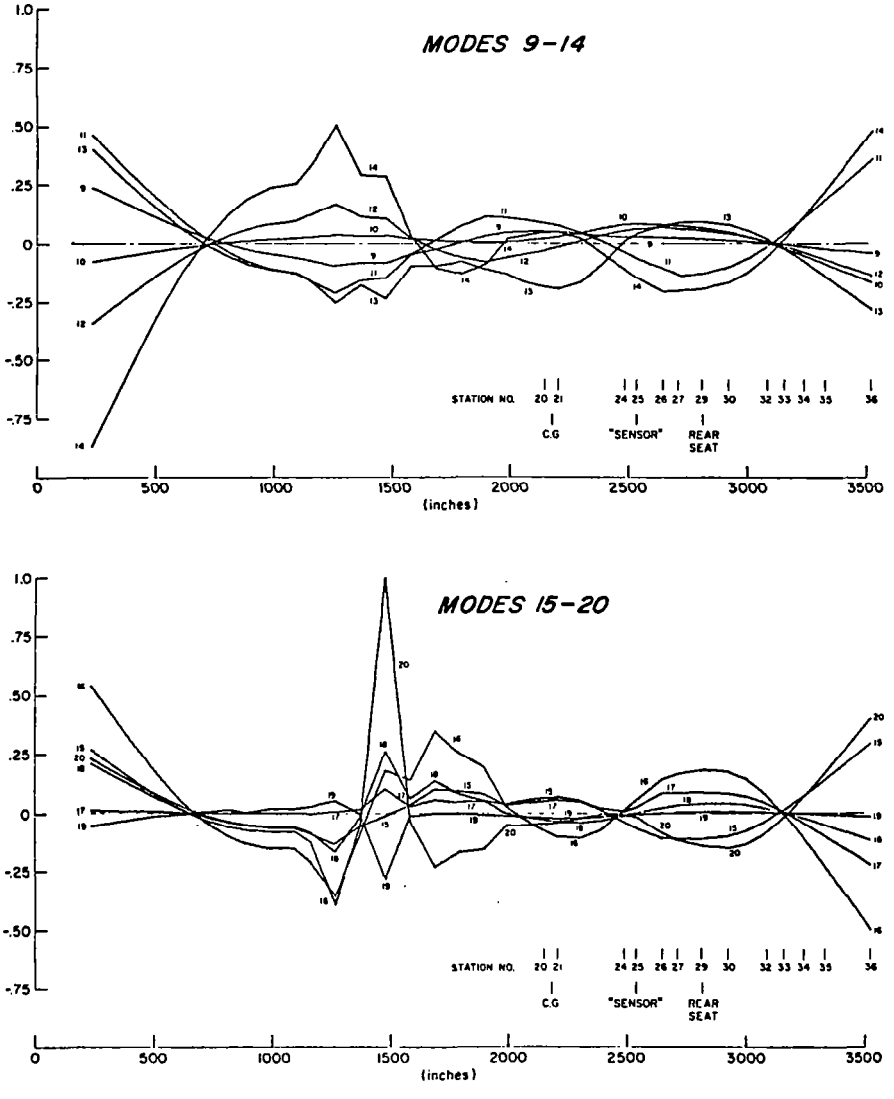

Figure 9

COMPARISON OF MODEL C WITH COMPLETE DISCRETE BOEING DATA

The number of elastic modes selected for final retention in the simplified model underwent a gradual increase from three to seven to ten largely to account for the acceleration response shown in Fig. 10. The reduced-order (10 mode) model "C" shown retains modes 3 to 6, 8, and 11 to 15, and is effected through progressive elimination of successive elastic modes by neglecting dynamic (s^2 and s) terms relative to (constant) stiffness terms in each successive modal column. The generalized coordinate to be eliminated, now characterized by only a stiffness term, is expressed in terms of the remaining coordinates. Notice that some of the retained modal equations are for higher frequency modes than those eliminated. This poses no mathematical problem, the progressive elimination of the equations in question proceeds as described above. However, there is no good physical rationale for neglecting the dynamic (s^2 and s) terms of certain lower frequency modes and retaining those for some higher frequency modes, except that it produces an excellent match as illustrated in Fig. 10, where the high-frequency behavior is reproduced with sufficient fidelity to permit accurate ride quality analyses to proceed on the basis of the reduced-order model.

This match is also based on simplified, "distributed" unsteady aerodynamics, meaning that for each degree of freedom, or matrix column, the corresponding flexible mode frequency was used to assign constant aerodynamics consistent with that value of reduced frequency.

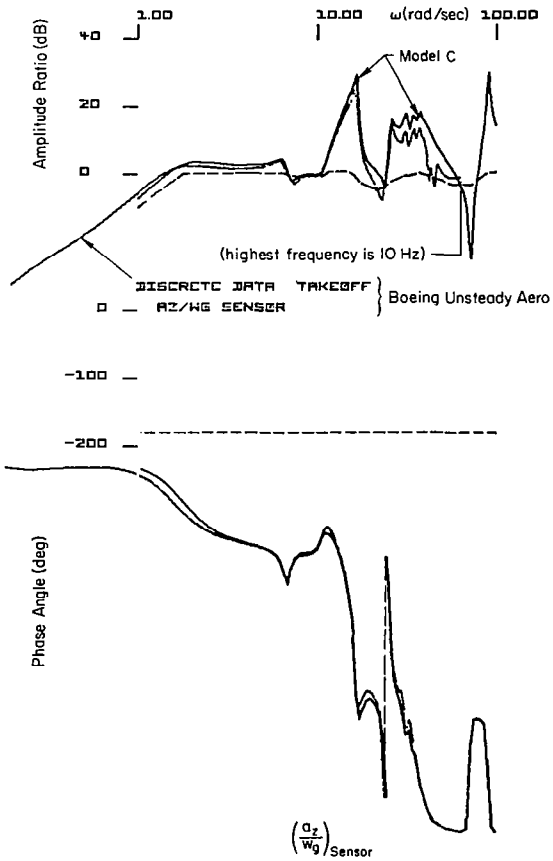

Figure 10

MODEL D TAKEOFF BODES OF PITCH ATTITUDE

A final correction was applied to eliminate perceived inconsistencies in the supplied numerical elevator inertial properties and produce the "final" (Fig. 11) model "D" attitude responses for two locations. The rear seat location provides the better sawtooth and is so labeled.

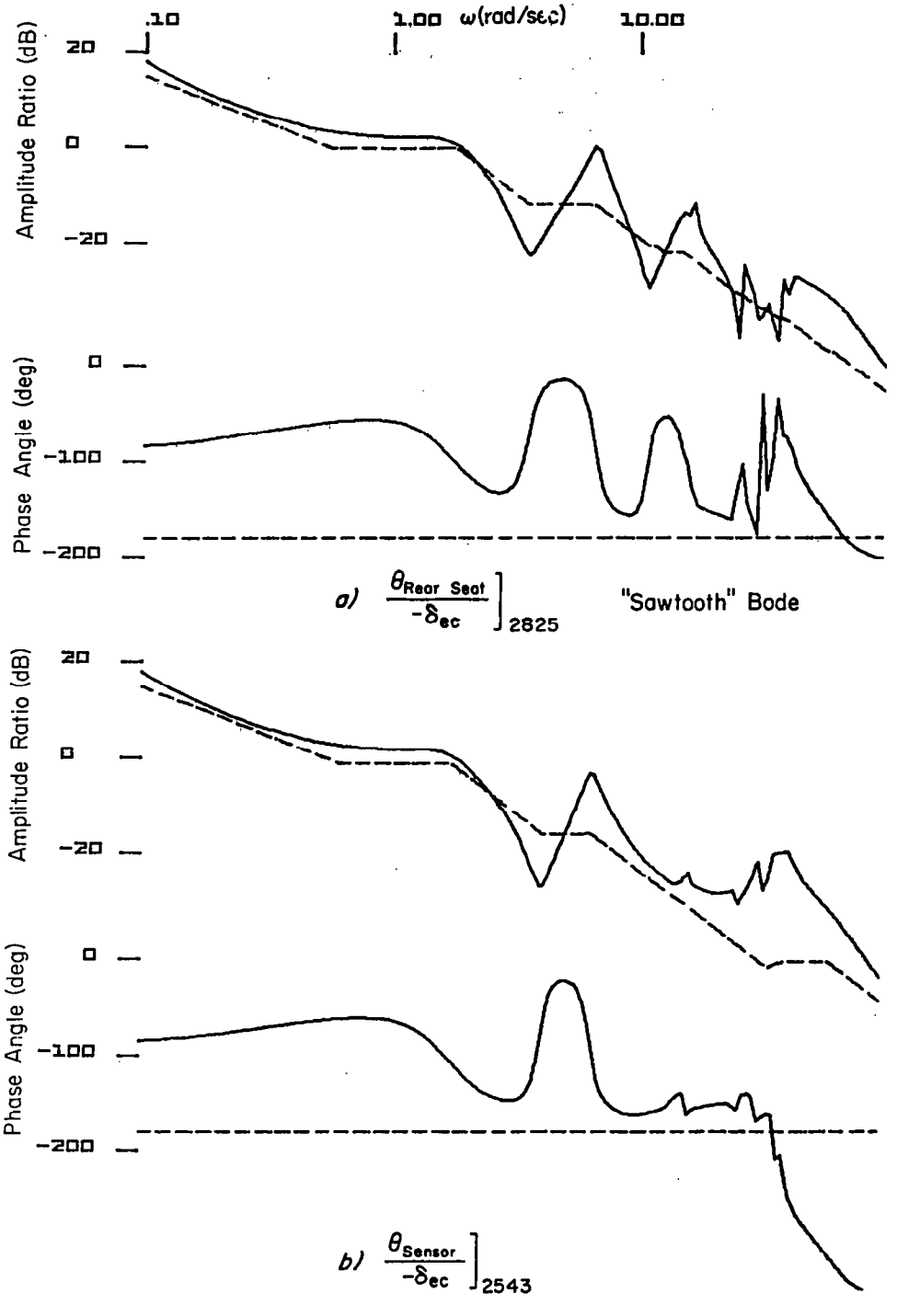

Figure 11

MODEL D TAKEOFF BODE WITH PITCH RATE GYRO

Figure 12 shows the Bode for a rate gyro, with typical dynamics, at the rear seat station with a suggested closure gain of 0.5.

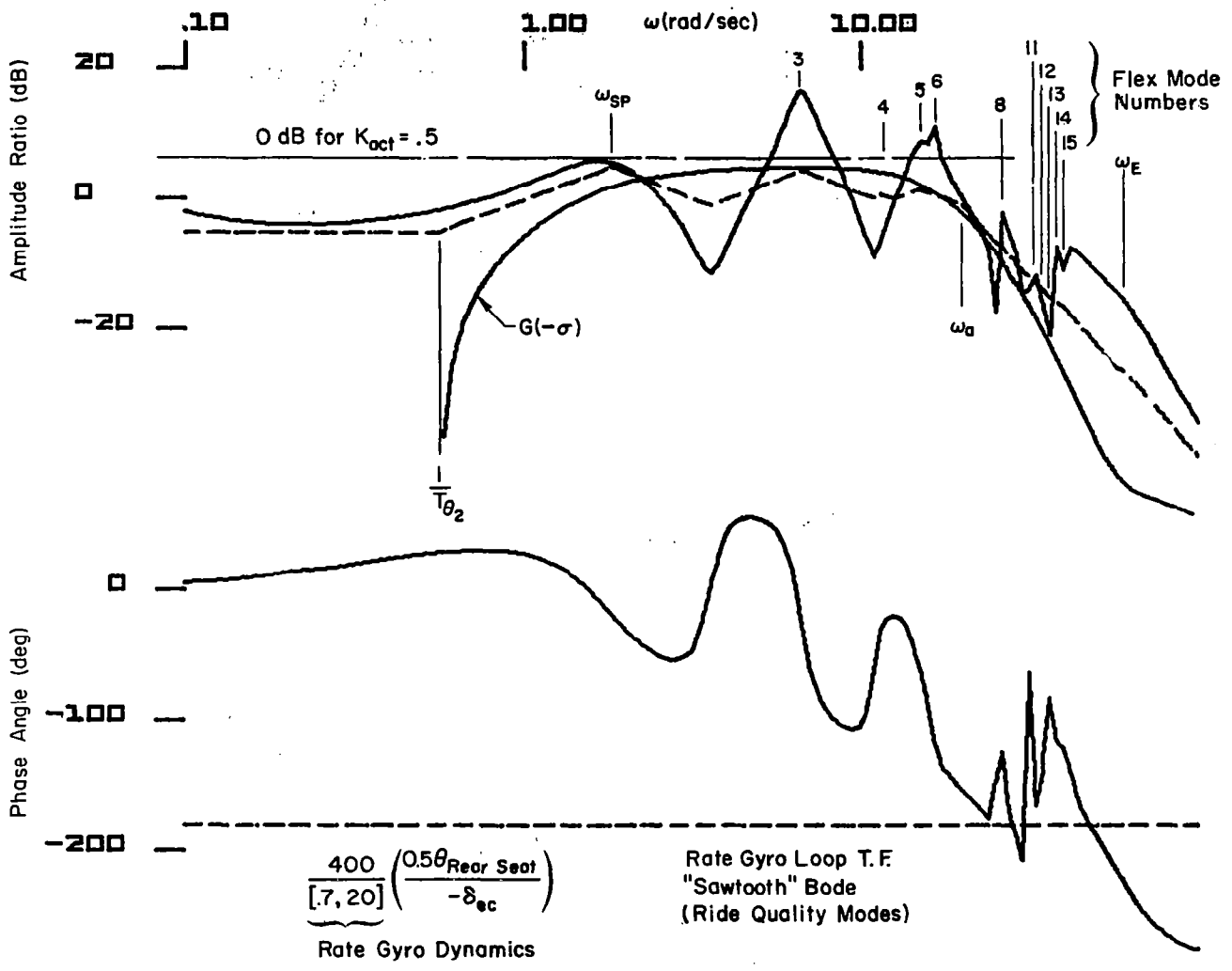

Figure 12

ROOT LOCUS PLOT OF FIGURE 12 SYSTEM

The corresponding root locus plot in Fig. 13 shows the resulting improved damping of all modes except 11, 13, and 14, which are slightly degraded.

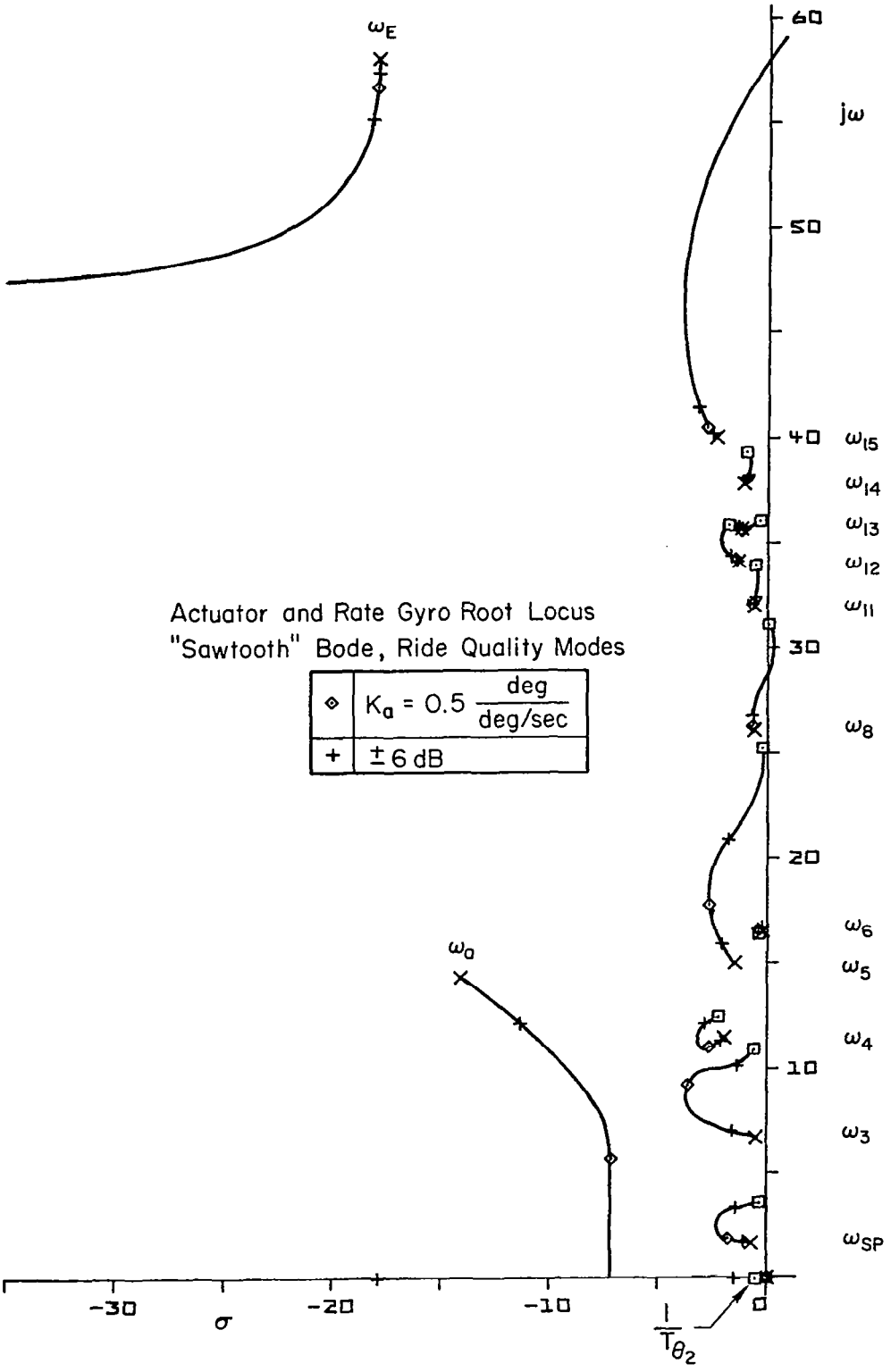

Figure 13

PILOT STATION AUGMENTED ATTITUDE RESPONSE TO ELEVATOR, $\frac{\theta'_{pilot}}{\delta_e}$

We also looked at a_z feedbacks to δ_e but they were not very effective in providing additional damping of the lower frequency modes. In fact, the higher frequency modes, 6, 8, and 11 to 15, are essentially unobservable by a centerline accelerometer. Accordingly, vertical acceleration feedback to the elevator appears to be unnecessary to slightly undesirable; it was therefore eliminated as a primary closure possibility. The remaining basic elevator control loop structure shown below is simple indeed (Fig. 14).

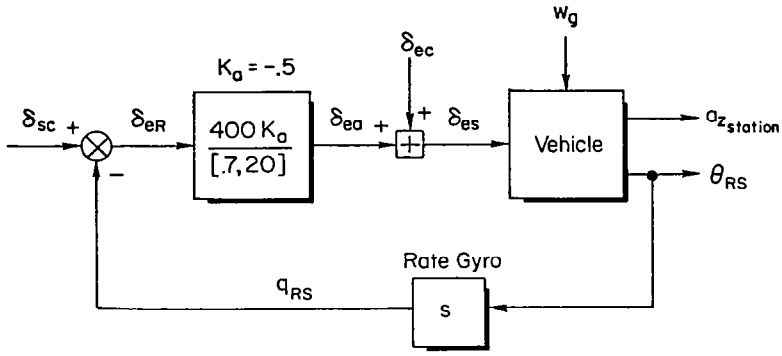

Figure 14

ELEVATOR CONTROL LOOP STRUCTURE

The basic FCS-augmented attitude response at the pilot's station to control inputs using this system is given in Fig. 15. The effective bandwidth, set in this case by a 6 dB gain margin requirement, is about 0.9 to 1.0 rad/sec which corresponds to satisfactory handling for this flight condition.

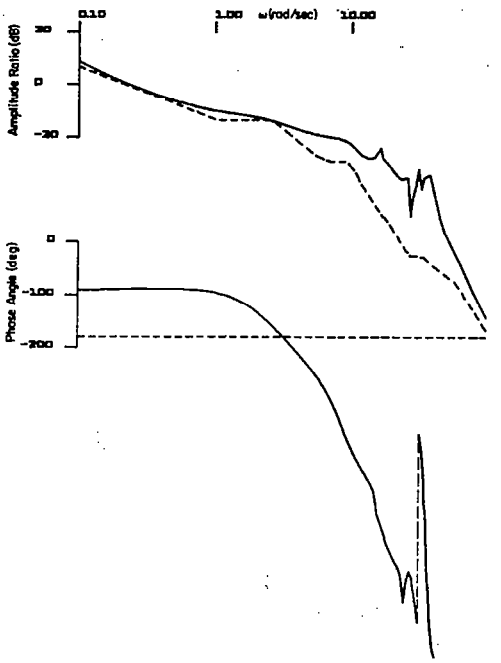

Figure 15

However, the pilot's station attitude response to a step input in Fig. 16 shows an effective time delay of about 0.55 sec, greater than allowable even using the most optimistic data. This quite large time delay is also apparent in the Fig. 15 phase characteristics (i.e., using the simple approximation $\tau\omega = 90$ deg $= 1.57$ rad where $\omega \sim \phi = 180$ deg, $\tau_{eff} \triangleq 1.57/3.2 \triangleq 0.49$). It is directly traceable to bending mode effects as shown at the bottom of Fig. 16, which shows only about a 0.10 sec delay in the pitch response at the rear seat where the mode slopes are all either basically smaller than, or opposite in sign to, those at the pilot station. Thus the difference is attributable to the natural change in sign of the mode slopes in going from the rear seat to the pilot's station. The change in sign is a result of the inherent bending mode shapes of a slender flexible body. In this sense, the associated additional time delay of the pilot's attitude response to a step control aft-surface input is fundamental. Before we decide what, if anything, can be done to eliminate or reduce such additional delay, we need to make further assessments.

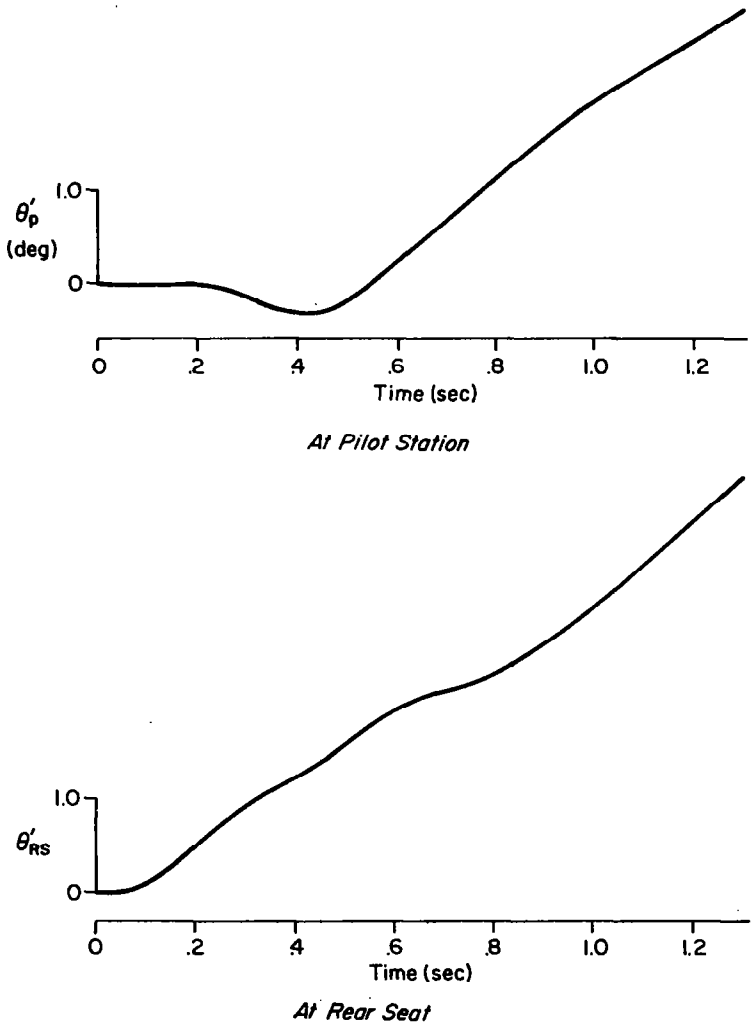

Figure 16

"SYNCHRONOUS" PIO POSSIBILITY

Relative to PIO proneness, the Fig. 15 pilot's attitude Bode is such that loop closure can be easily effected with pure gain adaptation on the part of the pilot. Accordingly, there is no tendency for the "PIO syndrome" which is characterized by required low-frequency lag adaptation for normal closed-loop operations. Such lag is an easy to accomplish, low-workload behavioral pattern described by pilots as a "smooth, trim-like control action." The trouble arises when, in an attempt to regain control after an upset or other stressful occurrence, the pilot regresses to a pure gain type of proportional control. Then the pilot-vehicle (with the suddenly changed pilot equalization) may temporarily have too small a gain margin at a "high" frequency oscillatory mode (short period or conceivably a flexible mode).

The lightly damped peak at about 16.5 rad/sec (Fig. 15) could conceivably be excited momentarily by "synchronous" pilot behavior at this frequency. The resulting PIO would not be unstable at the more probable lower gain shown in the fragmentary root locus of Fig. 17, but could have quite low damping. Of course, the level of pilot gain involved can only be sustained for a short time before the system diverges at the lower frequency corresponding to the -180 deg phase crossover in Fig. 15. Thus, at best, synchronous PIO would occur in "bursts" rather than in a sustained oscillation.

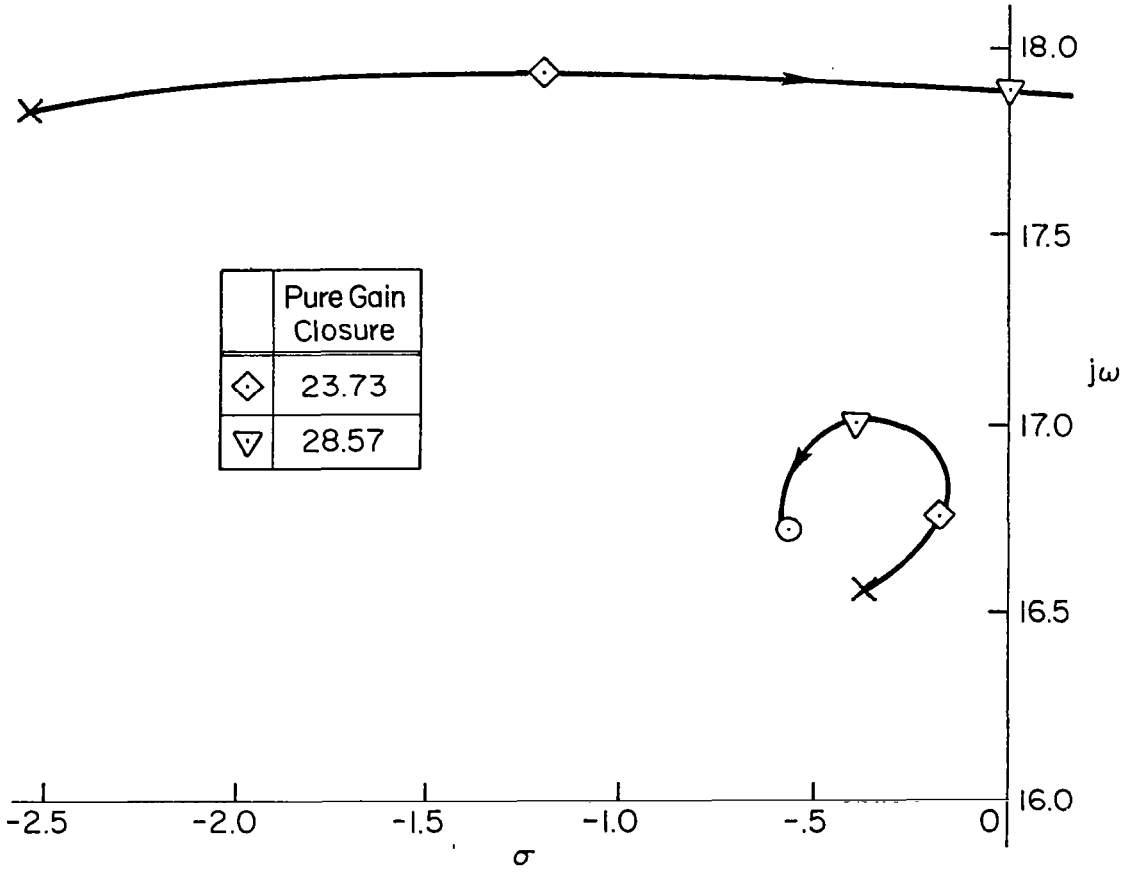

Figure 17

PILOT STATION ACCELERATION (a'_{z_p}) RESPONSE TO ELEVATOR INPUTS

With respect to vibration feedthrough to the pilot, the excitation at the pilot's station due to step and ramp elevator inputs is shown in Fig. 18. Clearly, the alleviating influence of a rate limited surface input is desirable to avoid the high-frequency ringing at about 40 rad/sec and to reduce the amplitude and frequency of the 16 rad/sec mode. However, for a 10-deg elevator ramped in at 30 deg/sec, the effective time delay increment (half of the time to ramp to 10 deg) is 0.17 sec. Therefore the effects of realistic surface rate limits will be to accentuate the effective time delay problem which is already possibly critical. A better solution to the vibration feedthrough problem than low surface rate saturation is desirable.

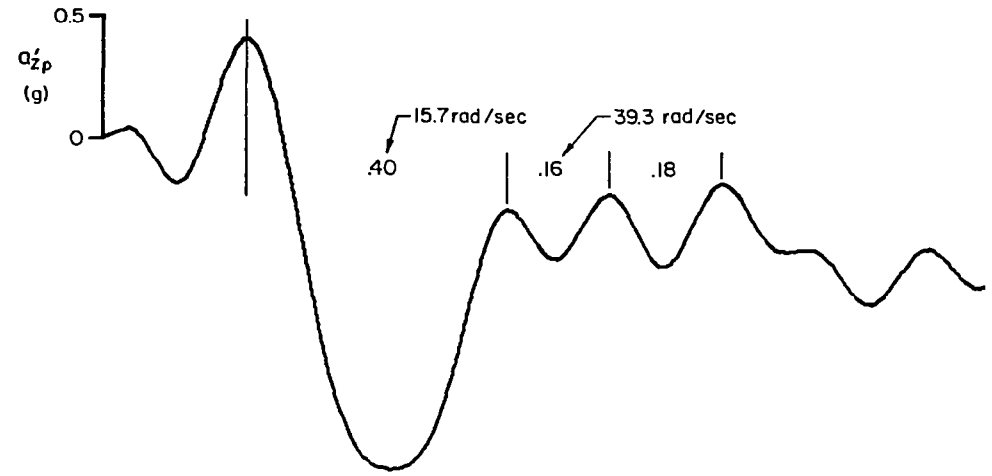

a) 10 deg Step

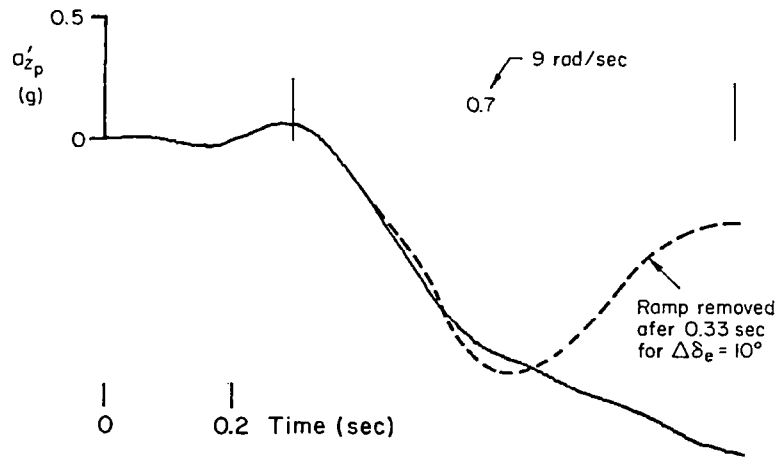

b) 30 deg/sec Ramp

Figure 18

$\left[\frac{a_z}{w_g}\right]'$ AMPLITUDES WITH SENSOR LOCATION

Turning now to ride qualities and Fig. 19, we have to recognize first that the usual Dryden turbulence spectra effectively flatten the asymptotic amplitude response to random gust inputs over almost the entire frequency range. This is indicated by the long dashed lines in Fig. 19 which represent the zero dB line for a σ_w unity gust, still leaving large spikes in the pilot's a_z response at about 16 and 36 rad/sec. As shown in the figure, these same spikes are generally evident along the entire cabin area. This means that ride quality is a general problem, not necessarily peculiar to pilot location. Accordingly, a general solution must be found. This could conceivably take one of two forms: use of a secondary control point to damp the offending modes or seat motion attenuation and damping.

The ride mode most evident in Fig. 19 is that at roughly 16 rad/sec, mode 6. The largest amplitude spike above the zero dB gust lines at 16 rad/sec is about 34 dB (at the rear node) or an amplification factor of 50. This is far too large to be effectively damped by passive seat suspension and cushioning systems.

Mode 6's three-dimensional character is predominantly of a wing torsional nature so it's not surprising that a centerline control has no effect on it. It is also clear that the wing lift due to such torsional deflection will apply more or less uniformly along the fuselage, which explains the Fig. 19 results. The obvious way to damp this motion is to use the outboard wing movable surfaces responding to motion also sensed at an outboard location. The Boeing data, unfortunately, do not cover symmetric aileron or flaperon inputs to the longitudinal mode, so this option remains as a possible future exercise.

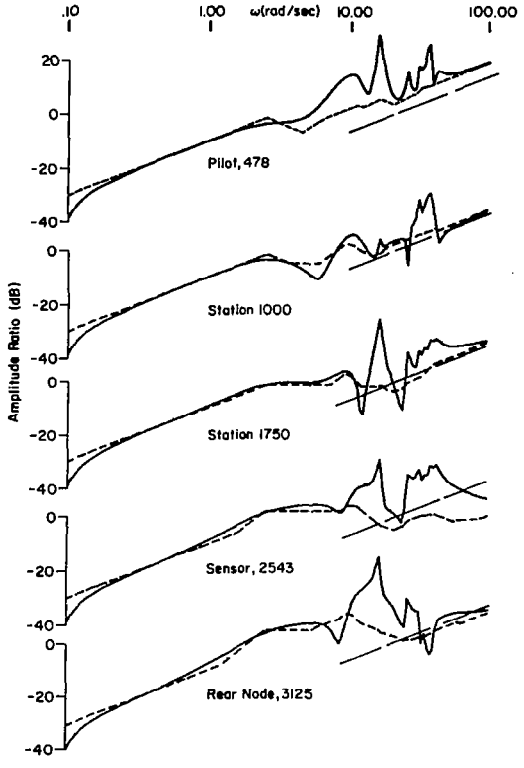

Figure 19

RESULTS AND CONCLUSIONS: GENERAL

- Systematically exposed all design-centered factors to consider (1)(Fig. 20)
  - Control system functions and roles
  - Flexible mode control principles
    - FCS criteria and desires for
      - Pilot-centered command and flying qualities
      - Ride qualities
      - Controller-centered requirements and design implications
  - Available design methodologies and selection of recommended methods
- Established fundamental requirements on effective vehicle characteristics (aircraft/controller combination) consistent with simple robust controllers -- i.e., pole-zero ordering (2)
- Translated above into system and subsystem requirements (1)
- Confirmed a simplified treatment of unsteady aerodynamics which compared very well with the complete treatment (3)
- Developed and demonstrated considerations for selective inclusion/deletion of significant/insignificant modes within reduced-order systems (3)
- Demonstrated systematic design/analysis methods to meet requirements; derived a very simple robust system (4)

(1) ASSEMBLED REQUIREMENTS AND DESIRES

(2) REITERATED A CENTRAL PRINCIPAL IN FLEXIBLE MODE CONTROL

(3) DERIVED AND UTILIZED A SIMPLIFIED FLEXIBLE AIRPLANE MODEL

(4) DEMONSTRATED SYSTEMATIC DESIGN METHODS

(5) IDENTIFIED CERTAIN PROBLEMS ENDEMIC TO FLEXIBLE VEHICLES OF TYPE STUDIED

Figure 20

CONCLUSIONS: SPECIFIC "PROBLEMS"

- The effective time delay in θ_p response to elevator appears to be a generic problem due to low-frequency bending mode(s) as seen at the pilot station (Fig. 21).
- Vertical acceleration feedthrough at the pilot's station can be reduced by lowering the saturation rate of the elevator. However, this adds to the θ response lag and may not be a viable solution.
- Vertical acceleration response to w_g is high in general and must be reduced for good ride qualities. Analysis indicates that secondary, outboard surface(s), and off-centerline located sensors offer a probable solution which should also decrease vertical acceleration feedthrough.
- The above "prominent" mode is also involved in "synchronous PIO" possibilities, but these are evident in the pilot's pitch attitude response and may or may not be reduced by the above-suggested secondary control surfaces.
- Because of its prominence in ride, synchronous PIO, and vibration feedthrough, response characteristics similar to those of the "prominent" mode are likely candidates for simulation research.

- τ_e IN θ_p RESPONSE TO ELEVATOR -- A GENERIC PROBLEM DUE TO LOW FREQUENCY BENDING MODE(S)
- VERTICAL ACCELERATION FEEDTHROUGH AT PILOT'S STATION
- VERTICAL ACCELERATION RESPONSE TO w_g IS HIGH IN GENERAL AND MUST BE REDUCED FOR GOOD RIDE QUALITIES
- THE ABOVE "PROMINENT" MODE IS ALSO INVOLVED IN "SYNCHRONOUS PIO" POSSIBILITIES
- BECAUSE OF ABOVE EFFECTS, RESPONSE CHARACTERISTICS OF THE "PROMINENT" MODE ARE LIKELY CANDIDATES FOR SIMULATION RESEARCH

Figure 21

RECOMMENDATIONS

- Expand present study to include off-center line symmetric controls (Fig. 22)
- Plan and conduct moving base simulation to investigate:
  - (a) Low-frequency time delays in pilot station attitude response associated with fuselage bending modes
  - (b) Motion feedthrough and potential synchronous PIO due to high-frequency centerline motion
- Develop more-automated means to achieve simple controllers which exhibit robust characteristics demonstrated herein, e.g.:

  Automated numerator synthesis for minimum (fixed-form) sensor/equalization complexes which assure desired zero, pole order, and permit maximum spacing between a limited (specified) number of zero, pole pairs

  Frequency domain optimal performance indices and procedures which preordain an optimal controller/aircraft combination satisfying the sawtooth Bode requirements

- STUDY OFF-CENTER LINE SYMMETRIC CONTROLS
- PLAN AND CONDUCT MOVING BASE SIMULATION TO INVESTIGATE:
  - (A) TIME DELAYS DUE FUSELAGE BENDING MODES
  - (B) FEEDTHROUGH AND POTENTIAL SYNCHRONOUS PIO DUE TO HIGH-FREQUENCY COCKPIT ACCELERATION
- DEVELOP MORE-AUTOMATED MEANS TO ACHIEVE SIMPLE, ROBUST CONTROLLERS

Figure 22

BIBLIOGRAPHY

1. Ashkenas, I. L., Magdaleno, R. E., and McRuer, D. T.: Flight Control and Analysis Methods for Studying Flying and Ride Qualities of Flexible Transport Aircraft, NASA CR-172201, August 1983.